Science in China Series D: Earth Sciences

The trend, seasonal cycle, and sources of tropospheric NO_2 over China during 1997－2006 based on satellite measurement

ZHANG XingYing†, ZHANG Peng, ZHANG Yan, LI XiaoJing & QIU Hong

Key Laboratory of Radiometric Calibration and Validation for Environmental Satellites, China Meteorological Administration (LRCVES/CMA), National Satellite Meteorological Center, China Meteorological Administration, Beijing 100081, China

The characteristics of spatial and temporal distribution of tropospheric NO_2 column density concentration over China are presented, on the basis of measurements from the satellite instruments GOME and SCIAMACHY. From these observations, monthly averaged tropospheric NO_2 variations are determined for the period of 1997 to 2006. The trend and seasonal cycle are also investigated. The possible source of tropospheric NO_2 over megacity area is discussed in this paper. The results show a large growth of tropospheric NO_2 over eastern China, especially above the industrial areas with a fast economical growth, such as, Yangtze Rive Delta region and Pearl River Delta region because of the prominent anthropogenic activity. There is a rapid increase of tropospheric NO_2 over megacities in China. For instance, Shanghai had a linear significant increase in NO_2 columns of ~20% per year (reference year 1997) in the period of 1997－2006, which is the rapidest increase among all the selected cities. The seasonal pattern of the NO_2 concentration shows a difference between the east and west in China. In the eastern part of China, an expected winter maximum in seasonal cycle is found because of the prominent anthropogenic activity and meteorological conditions. In the western part this cycle shows a NO_2 maximum in summer time, which is attributed to natural emissions, especially soil emissions and lightning. A quickly increasing vehicle population may contribute to the increase of tropospheric NO_2 over megacities in China for the remarkable correlation for vehicle population with tropospheric NO_2.

tropospheric NO_2, satellite instruments, trend, seasonal cycle and sources

Nitrogen oxides are emitted by all combustion processes and play a key part in the photochemically induced catalytic production of ozone, which results in summer smog and has increased levels of tropospheric ozone globally[1]. The photolysis of NO_2 leads to the photochemical formation of ozone (O_3) during daytime by a catalytic cycle involving organic peroxy radicals (RO_2), the hydroperoxy radical (HO_2), the hydroxyl radical (OH), volatile organic compounds (VOC) and carbon monoxide (CO). NO_2 can also react with O_3 to form the nitrate radical (NO_3), which is a strong oxidant and plays an important role in the nighttime chemistry. The main products of NO_2 in the troposphere are peroxyacetyl nitrate (PAN or $CH_3C(O)OONO_2$) and nitric acid (HNO_3). The stability of PAN in the atmosphere is highly temperature-dependent, and NO_2 is released with increasing temperature. Nitric acid is produced by daytime reaction of NO_2 with the OH radical or by nighttime formation of N_2O_5 followed by hydrolysis on aerosols[2,3]. Nitrogen dioxide (NO_2) as one of the most im-

Received May 28, 2007; accepted August 14, 2007
doi: 10.1007/s11430-007-0141-6
†Corresponding author (email: Zhangxingying@126.com)
Supported by the ESA-MOST "Drag-star" Program (Grant No. 2005AA132031XZ07) the National Basic Research Program of China "973" Project (Grant Nos. 2005CB422200x and 2006CB403702) and the Special Project for Climatic Change From Chinese Meteorological Administration (Grant No. CCSF2007-11)

portant species in tropospheric chemistry has attracted great attention of governments and scientists.

In addition, NO_2 also contributes to radiative forcing[4], because of its short lifetime, mainly locally and not on a global scale. However, its atmospheric chemistry controls in part the oxidizing capacity of the troposphere, as well as the abundance of ozone. Therefore NO_2 can also modify the radiative balance of the Earth through its influence not only on the tropospheric ozone chemistry, but also on the lifetimes of methane (CH_4) and other greenhouse gases[5].

Nitrogen oxides ($NO_x = NO + NO_2$) play an important role in atmospheric chemistry. The abundance of NO_2 in the troposphere is highly variable and influenced by both anthropogenic and natural emissions. NO_x has significant natural sources (e.g., lighting and soil emissions) and anthropogenic (e.g., biomass burning, fossil fuel combustion) sources. Global tropospheric NO_2 distributions are measured by the satellite instruments GOME (from 1995 to 2003) aboard ERS-2, SCIAMACHY (from 2002) aboard Envisat platform and OMI aboard EOS-AURA (from 2004)[6−9].

Recent studies on the tropospheric NO_2 columns show that the satellite measurements are suitable for improving emission inventories and air quality studies. Jaegle et al.[10] used GOME measurements over the Sahel to map the spatial and seasonal variations of NO_x, mainly caused by biomass burning and soil emissions. Martin et al.[11] used GOME measurements to derive a top-down emission inventory. The top-down inventory in combination with bottom-up emission inventory is used to achieve an optimized posterior estimate of the global NO_x emissions. Boersma et al.[12] used GOME measurements to estimate the global NO_x production from lightning by comparing modeled and measured spatial and temporal patterns of NO_2 in the tropics. In the work by Heue et al.[13], SCIAMACHY measurements are compared with an air quality model and ground measurements. They showed that SCIAMACHY measurements are able to monitor the air pollution over Europe and its day-to-day changes. Analysis of the satellite data has revealed the spatiotemporal distribution of tropospheric NO_2 on a global scale[6−8,14−16]. These studies have highlighted the areas of intense pollution in industrialized regions, emissions from biomass burning, soil emissions and lightning signatures.

Nitrogen oxide concentrations in many industrialized countries are expected to decrease[17], but rapid economic development has the potential to increase significantly the emissions of nitrogen oxides in parts of Asia[18−20]. China has one of today's fastest growing economies of the world. This increase in economic activity is accompanied by a strong increase of emissions of tropospheric pollutants and therefore leads to extra pressure on the environment. Here we present the tropospheric column amounts of nitrogen dioxide retrieved from two satellite instruments GOME[14,21] and SCIAMACHY[22] over the years 1997−2006.

1 Methods and sources of data

Measurements of the satellite instruments GOME and SCIAMACHY have been used to retrieve tropospheric columns of NO_2 from space[6−8,14], and validation of the data product used in this study has been performed[23].

GOME (Global Ozone Monitoring Experiment)[14,21] is a smaller version of SCIAMACHY (Scanning Imaging Absorption spectrometer for Atmospheric CHartographY)[22]. Both are passive remote-sensing instruments observing the back-scattered radiance from the earth and the extraterrestrial irradiance. GOME measures in nadir whereas SCIAMACHY observes in alternate limb and nadir viewing.

The GOME is a four-channel ultraviolet/visible spectrometer observing scattered sunlight in nadir viewing geometry[14]. GOME is part of the core payload of the ESA ERS-2 platform, which was launched in April 1995 and provided global coverage from August 1995 to June 2003. The instrument observes simultaneously the spectral region from 240−793 nm with a channel-dependent spectral resolution of 0.2 to 0.4 nm. The ground scene of GOME typically has a footprint of 320 km×40 km. With an across-track swath of 960 km, global coverage at the equator is achieved within three days.

SCIAMACHY was launched in March 2002 on ENVISAT. Nadir and limb data have been available since August 2002. The ultraviolet/visible nadir measurements of SCIAMACHY used here are similar to those from GOME, with the two main differences being the improved spatial resolution (60 km×30 km over most parts of the world) at reduced coverage. The latter is a result of the alternate limb nadir viewing, global coverage at the Equator being achieved in six days.

Satellite data are analyzed for tropospheric NO_2 in a four-step procedure. First, the NO_2 absorption averaged over all light paths contributing to the signal is determined using the Differential Optical Absorption (DOAS) method in the 425—450 nm regions [7]. In the second step, the stratospheric component is removed by subtracting the daily stratospheric NO_2 column simulated by the 3d-CTM SLIMCAT[24] for the time of the satellite overpass. To account for differences between model and measurement, the SLIMCAT data are scaled to the GOME data over a clean region (1808—2108 longitude). In a third step, a cloud screening is applied to removing those measurements with a cloud fraction of more than 0.2 as determined by the FRESCO algorithm[25]. The last step is the conversion of the tropospheric residual to a vertical tropospheric column by accounting for the vertical sensitivity of the measurement with the radiative transfer model SCIATRAN28. In this step, *a priori* information is needed on surface spectral reflectance29, surface altitude, aerosol loading and the shape of the vertical distribution of NO_2. The latter is taken from a run of the chemistry-transport MOZART-2 model[26] for 1997, which was used to determine monthly averaged air-mass factors on a 2.58×2.58 grid. Although the *a priori* assumptions used in the analysis have a significant impact on the retrieval results[7−9] the observed changes in NO_2 are unlikely to be affected because the same input was used for all years.

All the tropospheric NO_2 data from satellite used in this study were downloaded form the website, http://www.temis.nl/. And the concentration of NO_2 in ground produced from air pollution index (API) supported by EPA in Beijing and Shanghai during 2000 to 2006 was obtained from the websites (http://www.bjee.org.cn/api/index.php and http://www.envir.online.sh.cn/airnews/index.asp). API was converted to NO_2 concentration according to the following formula:

$$C = C_{low} + [(I - I_{low})/(I_{high} - I_{low})] \times (C_{high} - C_{low}),$$

where C is the concentration of NO_2 and I is the API value of NO_2. I_{high} and I_{low}, the two values most approaching to value I in the API grading limited value table (Table 1), stand for the value larger and lower one than I, respectively; C_{high} and C_{low} represent the NO_2 concentration corresponding to I_{high} and I_{low}, respectively.

Table 1 API grading limited value table

C=1.6I	when $0<I\leqslant 50$
C=0.8I+40	when $50<I\leqslant 100$
C=1.6I–40	when $100<I\leqslant 200$
C=2.85I–290	when $200<I\leqslant 300$
C=1.85I+10	when $300<I\leqslant 400$
C=1.9I-10	when $400<I\leqslant 500$

2 Results and discussion

2.1 Spatial and temporal distribution

We combined GOME and SCIAMACHY measurements to obtain a 10-year data for this study. The heavy pollution of NO_2 over the east of China is shown in Figure 1, especially the four regions: (1) Jingjinji region (2) Yangtze delta region; (3) Pearl River Delta region; and (4) Sichuan Basin. The average tropospheric NO_2 vertical column density over the east of China (110—123°E, 30—40°N) is about 9.3×10^{15} molec cm^{-2}, which is more than fifteen times to the value over the west of China (80—100°E, 30—40°N), 0.6×10^{15} molec cm^{-2}.

The temporal variations of the columns of tropospheric NO_2 above the region of the east of China and west of China are shown in more detail in Figure 2, where monthly averages are plotted from both GOME and SCIAMACHY. It can be seen clearly that there is distinct increase in tropospheric NO_2 over the east of China and no obvious change in the west of China in recent ten years. Figure 3 exhibits the rapid increase in tropospheric NO_2 over the east of China with about 0.82×10^{15} molec cm^{-2} a^{-1} during 1997 to 2006 (regression coefficient, R^2=0.96). The strong increase in tropospheric NO_2 emissions in the east of China is due to an increase in industry and traffic[27−29].

2.2 Seasonal variations

Since the lifetime of NO_x is longer in the winter, a NO_2 maximum is expected in the winter [15]. Figure 2 shows a monthly average of tropospheric NO_2 vertical columns over the east and west of China. It can be seen that in the east of China a seasonal NO_2 maximum is found according to the expected winter maximum, but in the west of China a NO_2 maximum during summertime is found. The reason for the difference existed in the east and west of China will be discussed in detail in Section 2.4

Figure 4 show the fours seasons (spring: Mar.—Apr.—May; summer: Jun.—Jul.—Aug.; autumn: Sep.—Oct.—Nov.; winter: Dec.—Jan.—Feb.) variation of tropospheric NO_2 over east and west of China respectively during the recent ten years. In the east of China, the four

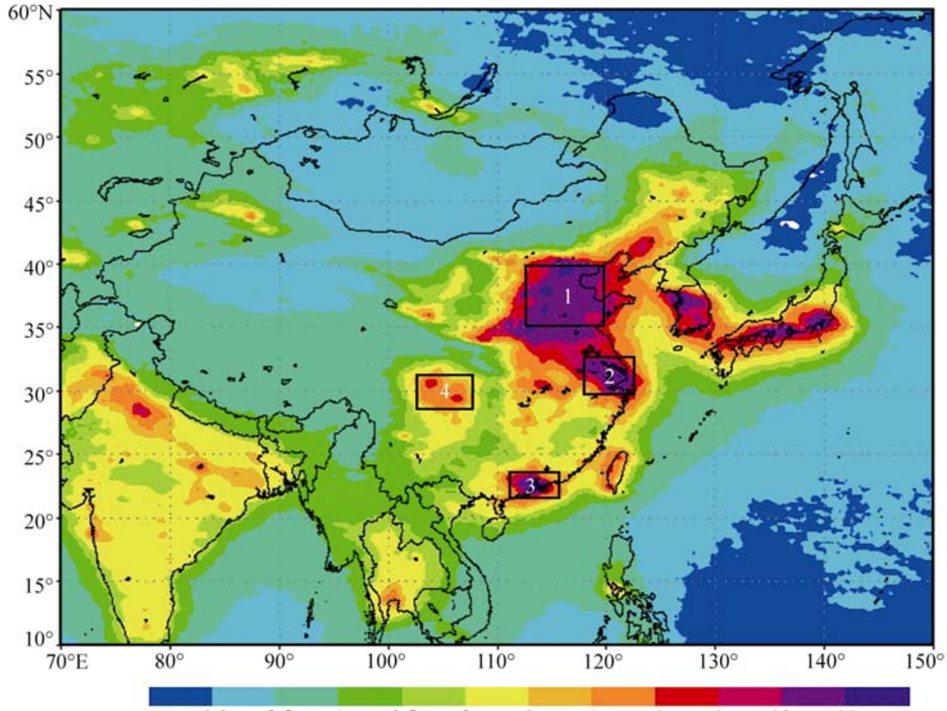

Figure 1 Tropospheric NO_2 vertical columns averaged between 1997 and 2006. (1) Jing-Jin-Ji region (2) Yangtze delta region; (3) Pearl River Delta region; (4) Sichuan Basin.

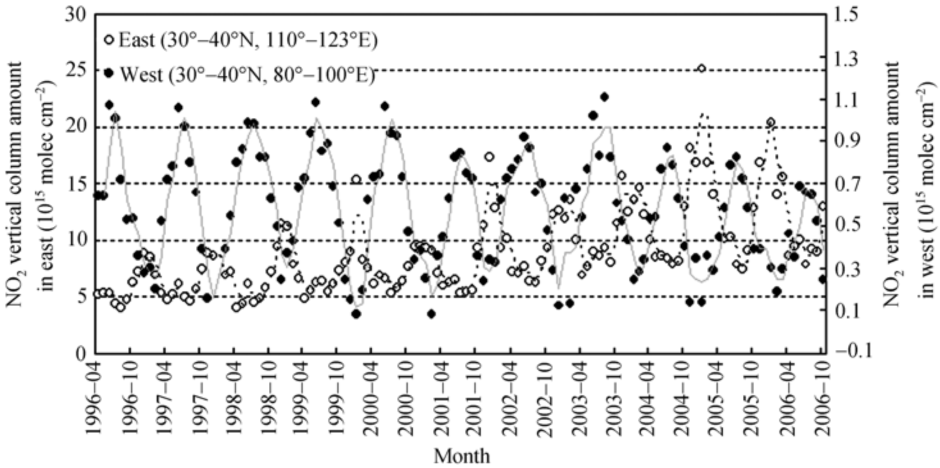

Figure 2 Monthly variations of tropospheric NO_2 over the east and west of China.

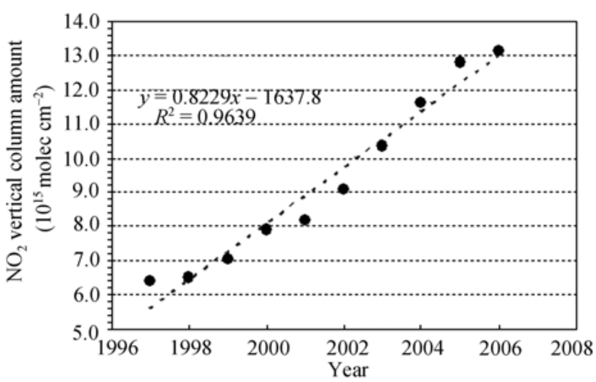

Figure 3 Temporal evolution of tropospheric NO_2 vertical columns density over the east of China.

seasons increase obviously with the regression coefficient about 0.9, especially the winter (1.15×10^{15} molec cm^{-2} a^{-1}) with the strongest increase. Over the west of China, there is a little decrease from 2001 (Figure 4(b)) with non-linear trend. But for the winter, the trend is hardly movement in this period. The order of the vertical column density level of tropospheric NO_2 for the different seasons over the east of China is: winter>spring> autumn>summer; and for the west the order is reversed with the east with summer > spring > autumn > winter. It can be seen clearly that there is distinct seasonal charac-

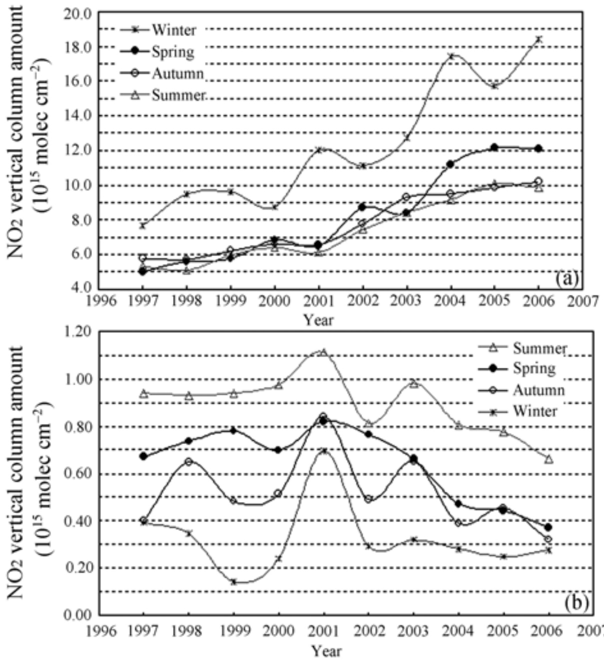

Figure 4 Seasonal variations of tropospheric NO_2 over the east and west of China. (a) East of China; (b) west of China.

teristic between the east and west because of the different pollution sources and location geography.

2.3 Characteristics of tropospheric NO_2 over megacity in China

Table 2 shows the trend estimates and start values of tropospheric NO_2 for some megacities in China, where the population is more than 10 million. A yearly growth is determined in terms of percentage with respect to the start value in 1997 to indicate the increase of the NO_2 column. It should be noted that this percentage is given relative to the start value in 1997 because we applied a linear model. Shanghai is the fastest growing industrial areas, which is reflected in a large growth in NO_2. The growth rate of tropospheric NO_2 in Shanghai is the largest among those megacities, since Shanghai is the economic centre of China including a harbor and industrial activities that are stimulated by the Chinese government. The trend over background (86±0.5°E×40±0.5°N) is not significant in this period.

The temporal development of the NO_2 column for the megacities and background area is shown in Figure 5 relative to the value measured in 1997. It can be seen clearly that all the values are on the increase except for background area. It is economic centre and industrial activities in megacity in China including high population density, thus inducing rapid increase of tropospheric NO_2.

Table 2 Tropospheric NO_2 vertical columns over megacities in China

	Mean concentration NO_2 in 1997 (10^{15} molec cm^{-2})	Linear trend in NO_2 (10^{15} molec cm^{-2} a^{-1})	Growth (reference year 1997)
Beijing	12.7	2.3	18.0
Tianjin	13.0	2.0	20.0
Shanghai	10.1	1.7	13.1
Guangzhou	10.7	0.9	16.4
Chengdu	3.8	0.7	19.1
Chongqing	3.7	0.7	19.0
Background (86±0.5°E× 40±0.5°N)	0.6	−0.03	−5.2

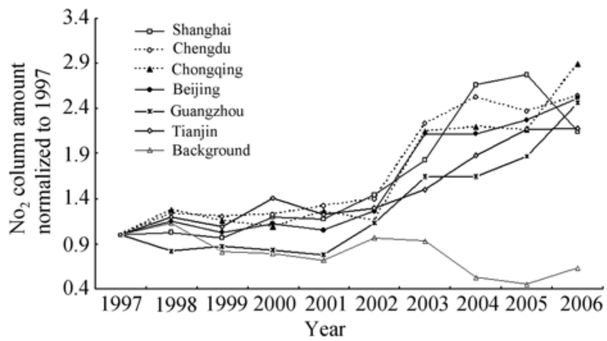

Figure 5 Temporal evolutions of tropospheric NO_2 columns for magacities areas.

2.4 Source appointment

Based on the population distribution in China (http://www.agro-labs.ac.cn/21c/jpg/5-1-5.jpg), it could be clearly seen that those emissions of tropospheric NO_2 are concentrated on the densely populated and industrialized eastern part of China. The western part of China has a low population density[29]. As a consequence natural emissions are expected to dominate the tropospheric column. But in the north and west, above the large city (Urumqi), a winter maximum is found, which strengthens the idea that the summer maximum in NO_2 over the rest of west China is caused by natural emissions.

The NO_2 lifetime is on the order of one day depending on many factors like meteorological conditions, photolysis timescale and OH concentrations. The combination of the variability in meteorological conditions, chemistry and emissions leads to a seasonally dependent NO_2 concentration with an expected maximum of NO_2 in wintertime in regions with strong anthropogenic emissions. In wintertime, the anthropogenic emissions are expected to be higher because of heating of buildings, as shown for China by Streets et al.[19]. Beirle et al.[15] found variability with a weekly pattern in the NO_2 concentration above Europe, related to reduce anthropogenic emissions during the weekend. In Figure 2, it could be clearly seen that there is an expected maximum of NO_2 in wintertime in the east of China, which is strong anthropogenic emissions. And the summer maximum in NO_2 over the west of China is caused by natural emissions as discussion above.

Some researchers measured lightning flash densities by the Optical Transient Detector (OTD) (http://thunder.msfc.nasa.gov/otd/). A comparison between the summer and winter flash densities can indicate that lightning above China especially occurs during summertime when the flash rate is about 5—6 times higher than during wintertime[30]. The contribution of lightning to the tropospheric NO_2 column is strongest in the tropics, with an estimated maximum of 0.4×10^{15} molec/cm^2[31]. Because the difference between summer and winter tropospheric columns is typical of the order 1.0×10^{15} molec/cm^2, lightning alone cannot account for all the natural emissions in west China. Duncan et al.[32] show that there is no biomass burning in the western part of China. In the work by Yienger and Levy (1995) it is suggested that in remote and agricultural regions soil emissions contribute 50% to the total NO_x budget and that in July these percentages can rise to more than 75%[33]. Yienger and Levy[33] also suggested that soil NO_x emissions are temperature-dependent, soil- dependent and precipitation-dependent. A higher surface temperature leads to more NO_x emissions, which would explain higher NO_x concentrations in summer time.

As the increase emission of tropospheric NO_2 over megacity in China, we selected two typical cities Beijing and Shanghai for study. In order to compare with the data from the ground measurement, the ground NO_2 concentrations in Beijing and Shanghai have been collected. The positive correlation between ground NO_2 concentration and tropospheric NO_2 column has been found in these two cities (see Figure 6), which demonstrates that the NO_2 emission from the ground contributes much to tropospheric NO_2 over the megacity.

Another light sight has been generated in the study on vehicles population with the tropospheric NO_2 column in megacity. The number of vehicles population has rapidly increased from 1.1 million in 1997 to 2.9 million in 2006 in Beijing, and the number will be about 320 million in 2008 (http://www.tranbbs.cn/Html/TechArticleData/0703121247921.html). Figure 7 shows the remarkable positive relationship between vehicles population and tropospheric NO_2 column in Beijing with regression coefficient R^2=0.9 (see Figure 8) during 1997 to 2006. Aggressive measures were instituted by the Beijing municipal authorities to restrict vehicular traffic in the Chinese capital during the recent Sino-African Summit[34]. The reductions in associated emissions of NO_x were detected by the Dutch-Finnish Ozone Monitoring Instrument (OMI) aboard the Aura satellite. They conclude that traffic restrictions implemented during the Sino-African Summit were remarkably successful in reducing emissions of NO_x by as much as 40%[34]. It could conclude that increasing vehicles population with the exhausted gas could contribute to the observed increase of tropospheric NO_2.

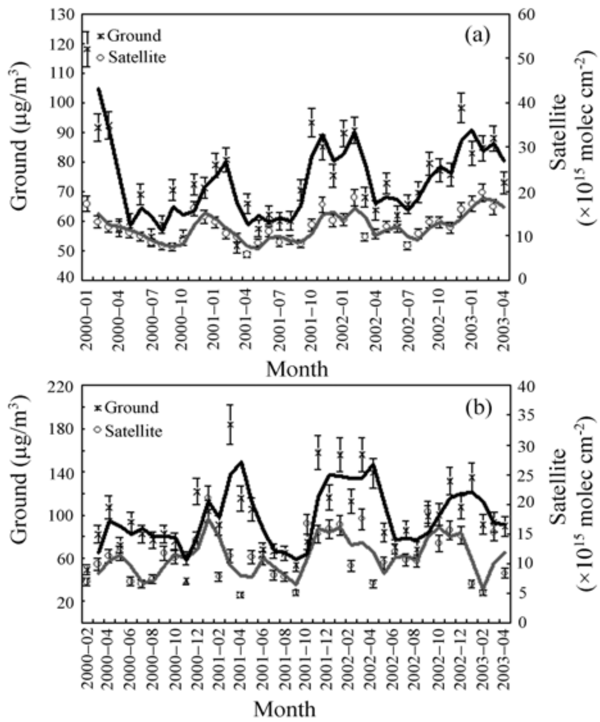

Figure 6 Variations of ground NO_2 concentration and tropospheric NO_2 column in megacity. (a) Beijing; (b) Shanghai.

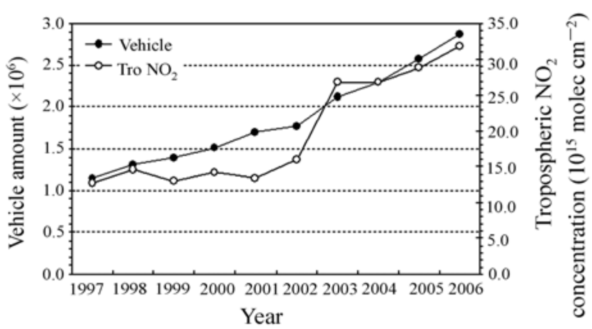

Figure 7 Variations of vehicles population and tropospheric NO_2 column in Beijing.

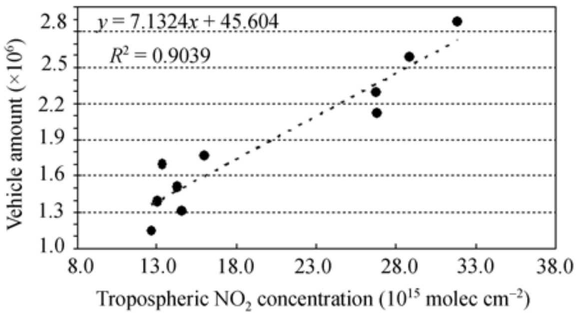

Figure 8 Relationship between vehicles population and tropospheric NO_2 column in Beijing.

3 Conclusions

The tropospheric NO_2 columns measured by GOME and SCIAMACHY during 1997 to 2006 have been used for the study for trend, seasonal cycle and sources analysis of tropospheric NO_2 over China. The geographic annual average distribution of tropospheric NO_2 over China was studied. The eastern part of China, a high populated and industrial area has high tropospheric NO_2 columns. And in western China, as there is nearly no anthropogenic activity, a low tropospheric NO_2 column has been found.

In the eastern part of China, an expected winter maximum in seasonal cycle is found due to the prominent anthropogenic activity and meteorological conditions. In the western part this cycle shows a NO_2 maximum in summertime, which is attributed to natural emissions, especially soil emissions and lightning.

Over megacities areas, the tropospheric NO_2 columns show increasing emission in the last ten years and there is no significant change in background areas in China. Shanghai is the fastest growing megacity with a yearly increase of ~20% according to 1997.

The ground NO_2 concentrations show the positive correlation with its tropospheric NO_2 column over megacity. Furthermore, the vehicles population in Beijing shows remarkable positive relationship with its tropospheric NO_2 columns, which proves that prominent anthropogenic activity and increasing vehicles exhausted gas could contribute to the observed increase of tropospheric NO_2.

The rapid increases in NO_2 observed by GOME and SCIAMACHY over the last decade demonstrate that the expanding Chinese economy has significantly increased air pollution.

The authors would like to thank for the data of tropospheric NO_2 provided by the TEMIS web site hosted by KNMI, the Netherlands.

1 Volz A, Kley D. Evaluation of the Montsouris series of ozone measurements made in the nineteenth centu ry. Nature, 1988, 332: 240－242
2 Dentener F J, Crutzen P J. Reaction of N_2O_5 on tropospheric aerosols: Impact on the global distributions of NO_x, O_3, and OH. J Geophys Res, 1993, 98: 7149－7163
3 Jacob D J. Introduction to Atmospheric Chemistry. Princeton: Princeton Univ. Press, 1999
4 Solomon S, Portmann R W, Sanders R W, et al. On the role of nitrogen dioxide in the absorption of solar radiation. J Geophys Res, 1999, 104: 12047－12058
5 Houghton J T. Intergovernmental Panel on Climate Change, Climate Change 2001: The Scientific Basis, Contribution of Working Group I to the Third Assessment Report of the IPCC. New York: Cambridge Univ. Press, 2001
6 Leue C, Wenig M, Wagner T, et al. Quantitative analysis of NO_x emissions from Global Ozone Monitoring Experiment satellite image sequences. J Geophys Res, 2001, 106: 5493－5505[DOI]
7 Richter A, Burrows J P. Retrieval of tropospheric NO_2 from GOME measurements. Adv Space Res, 2002, 29(11): 1673－1683[DOI]
8 Martin R V, Chance K, Jacob D J, et al. An improved retrieval of tropospheric nitrogen dioxide from GOME. J Geophys Res, 2002, 107 (D20), 4437, doi: 10.1029/2001JD001027
9 Boersma K F, Eskes H J, Brinksma E J, et al. Error analysis for tropospheric NO_2 retrieval from space. J Geophys Res, 2004, 109, D04311, doi: 10.1029/2003JD003962
10 Jaegle L, Martin R V, Chance K, et al. Satellite mapping of rain-induced nitric oxide emissions from soils. J Geophys Res, 2004,109, D21310, doi: 10.1029/2004JD004787
11 Martin R V, Jacob D J, Chance K V, et al. Global inventory of nitrogen dioxide emissions constrained by space-based observations of NO_2 columns. J Geophys Res, 2003, 108(D17), 4537, doi: 10.1029/2003JD003453
12 Boersma K F, Eskes H J, Meijer E W, et al. Estimates of lightning NO_x production from GOME satellite observations. Atmos Chem Phys Disc, 2005, 5:3047– 3104
13 Heue K-P, Richter A, Bruns M, et al. Validation of SCIAMACHY tropospheric NO_2-columns with AMAXDOAS measurements. Atmos Chem Phys, 2005, 5: 1039－1051
14 Burrows J, Weber M, Buchwitz M, et al. The Global Ozone Monitoring Experiment (GOME): Mission concept and first scientific results. J Atmos Sci, 1999, 56: 151－175[DOI]
15 Beirle S, Platt U, Wenig M, et al. Weekly cycle of NO_2 by GOME measurements: A signature of anthropogenic source. Atmos Chem Phy, 2003, 3: 2225－2232
16 Kunhikrishnan T, Lawrence M G, Kuhlmann R, et al. Analysis of tropospheric NOx over Asia using the model of atmospheric transport and chemistry (MATCH-MPIC) and GOME-satellite observations.

Atmos Environ, 2004, 38: 581－596
17 Leveled G, Tarrason L, Tørseth K, et al. EMEP Assessment Part I. European Perspective the Cooperative Programme for Monitoring and Evaluation of the Long-range Transmission of Air Pollutants in Europe, (Norwegian Meteorological Institute, Oslo), 2004. 48－51
18 Streets D G, Waldhoff S T. Present and future emissions of air pollutants in China: SO_2, NO_x, and CO. Atmos Environ, 2000, 34: 363－374
19 Streets D G, Bond T C, Carmichael G R, et al. An inventory of gaseous and primary aerosol emissions in Asia in the year 2000. J Geophys Res, 2003, 108(D21): 8809, doi: 10.1029/2002JD003093
20 Akimoto H. Global air quality and pollution. Science, 2003, 302: 1716－1719
21 European Space Agency. GOME Global Ozone Measuring Experiment Users Manual, ESA SP-1182, ESA/ESTEC, Noordwijk, 1995
22 Bovensmann H, Burrowsa J P, Buchwitza M, et al. SCIAMACHY—Mission objectives and measurement modes. J Atmos Sci, 1999, 56: 127－150[DOI]
23 Petritoli A, Bonasoni P, Giovanelli G, et al. First comparison between ground-based and satellite-borne measurements of tropospheric nitrogen dioxide in the Po basin. J Geophys Res, 2004,109, D15307, doi: 10.1029/2004JD004547
24 Chipperfield M P. Multiannual simulations with a three-dimensional chemical transport model. J Geophys Res, 1999, 104: 1781－1805
25 Koelemeijer R B, Stammes A, Hovenier P, et al. A fast method for retrieval of cloud parameters using oxygen A band measurements from the Global Ozone Monitoring Experiment. J Geophys Res, 2001, 106: 3475－3490
26 Horowitz L W, Horowitz L W, Walters S, et al. A global simulation of tropospheric ozone and related tracers: description and evaluation of MOZART (version 2). J Geophys Res, 2003, 108 (D24), 4474, doi: 10.1029/2002JD002853.
27 Wang Y X, McElroy M B, Wang T, et al. Asian emissions of CO and NOx: Constraints from aircraft and Chinese station data. J Geophys Res, 2004, 109(D24304) doi: 10.1029/2004JD005250
28 Richter A, Burrows J P, Nüß H, et al. Increase in tropospheric nitrogen dioxide over China observed from space. Nature, 2005, 437: 129－132[DOI]
29 Van der A R, Peters D H M U, Eskes H, et al. Detection of the trend and seasonal variation in tropospheric NO_2 over China. J Geophys Res, 2006, 111, D12317, doi: 10.1029/2005JD006594
30 Christian H J, Blakeslee R J, Boccippio D J, et al. Global frequency and distribution of lightning as observed from space by the Optical Transient Detector. J Geophys Res, 2003, 108(D1), 4005, doi: 10.1029/2002JD002347
31 Edwards D P, Lamarque J F, Attié J L, et al. Tropospheric ozone over the tropical Atlantic: A satellite perspective. J Geophys Res, 2003, 108(D8), 4237, doi: 10.1029/2002JD002927
32 Duncan B N, Martin R V, Staaudt A C, et al. Interannual and seasonal variability of biomass burning emissions constrained by satellite observations. J Geophys Res, 2003, 108(D2), 4100, doi: 10.1029/2002JD002378
33 Yienger J J, Levy H. Empirical model of global soil biogenic NO_x emissions. J Geophys Res, 1995, 100: 11447－11464[DOI]
34 Wang Y, McElroy M B, Boersma K F, et al. Traffic restrictions associated with the Sino-African summit: Reductions of NO_x detected from space. Geophys Res Lett, 2007, 34, L08814, doi: 10.1029/2007GL029326